

RESEARCH

Open Access



# Positive regulation of ataxia-telangiectasia-mutated protein (ATM) by E2F transcription Factor 1 (E2F-1) in cisplatin-resistant nasopharyngeal carcinoma cells

Zun-Yan Zhou, Ji-Yuan Yang, Cheng-Ze Shao, Fei Luo and Wei Du\*

## Abstract

**Objective:** To explore the mechanism of E2F transcription Factor 1 (E2F-1)-mediated ataxia-telangiectasia-mutated protein (ATM) in cisplatin (DDP)-resistant nasopharyngeal carcinoma (NPC).

**Methods:** E2F-1 and ATM expression was assessed in DDP-resistant NPC cell lines (CNE2/DDP and HNE1/DDP) and parental cells. Then, DDP-resistant NPC cells were transfected with control shRNA (short hairpin RNA) or E2F-1 shRNAs with or without ATM lentiviral activation particles. The half maximal inhibitory concentration (IC<sub>50</sub>) was evaluated by 3-[4,5-dimethylthiazol-2-yl]-2,5 diphenyl tetrazolium bromide (MTT) assay, and the cell cycle and cell proliferation were measured by flow cytometry and EdU staining, respectively. In addition, the expression of genes and proteins was quantified by quantitative reverse-transcription polymerase chain reaction (qRT-PCR) and western blotting, respectively.

**Results:** Both E2F-1 and ATM expression in DDP-resistant NPC cells was much higher than that in parental cells. E2F-1 shRNA reduced ATM expression in DDP-resistant NPC cells, but ATM overexpression had no significant effect on E2F-1. ATM overexpression enhanced DDP resistance in DDP-resistant NPC cells with increased IC<sub>50</sub> values, which was reversed by E2F-1 inhibition. Meanwhile, ATM overexpression resulted in upregulation of ABCA2 and ABCA5 in DDP-resistant NPC cells, induced elevations in the transition of the cells into S-phase, and increased cell proliferation with enhanced expression of cyclin E1, CDK2, and Ki67, which was reversed by E2F-1 shRNAs.

**Conclusion:** Downregulation of E2F-1, possibly by regulating ATM, could block the cell cycle in the G1 phase and reduce the proliferation of CNE2/DDP cells, thereby reversing the resistance of human NPC cells to DDP.

**Keywords:** Nasopharyngeal carcinoma, E2F transcription Factor 1, Ataxia-telangiectasia-mutated protein, Cisplatin, Resistance

## Introduction

As one of the most common malignant tumors in the world, nasopharyngeal carcinoma (NPC) mainly occurs in the upper and sidewalls of the nasopharyngeal

cavity [1, 2]. The prevalence and mortality rate of NPC, on the basis of the data available from the International Agency for Research on Cancer (IARC)/World Health Organization (WHO) in 2020, have reached 1.7% and 1.0%, respectively, worldwide in both sexes and all ages; moreover, NPC has been ranked third in all malignant tumors, with a death rate of 34,810 in China (<https://gco.iarc.fr/today/>). According to the classification standard

\*Correspondence: duweiweidu\_6587@163.com  
Department of Oncology, The First People's Hospital of Jingzhou,  
Jingzhou 434000, China



© The Author(s) 2022. **Open Access** This article is licensed under a Creative Commons Attribution 4.0 International License, which permits use, sharing, adaptation, distribution and reproduction in any medium or format, as long as you give appropriate credit to the original author(s) and the source, provide a link to the Creative Commons licence, and indicate if changes were made. The images or other third party material in this article are included in the article's Creative Commons licence, unless indicated otherwise in a credit line to the material. If material is not included in the article's Creative Commons licence and your intended use is not permitted by statutory regulation or exceeds the permitted use, you will need to obtain permission directly from the copyright holder. To view a copy of this licence, visit <http://creativecommons.org/licenses/by/4.0/>. The Creative Commons Public Domain Dedication waiver (<http://creativecommons.org/publicdomain/zero/1.0/>) applies to the data made available in this article, unless otherwise stated in a credit line to the data.

of the WHO, NPC can be categorized into keratinizing squamous cell carcinoma (KSCC), nonkeratinizing differentiated carcinoma (NKDC), and nonkeratinizing undifferentiated carcinoma (NKUC), with common clinical features of nasal obstruction, epistaxis, hearing loss and stuffy ear, diplopia, and headache [3, 4]. Moreover, the majority of patients with advanced disease do not benefit from surgery with poor prognosis [5, 6]. Radiotherapy dominates the treatment strategies for NPC in accordance with the guidelines of the National Comprehensive Cancer Network (NCCN) and is sometimes combined with chemotherapy, depending on the condition of the patient [7]. Among all drugs for the treatment of NPC, cisplatin (DDP) and 5-fluorouracil (5-FU) have been found to be the most effective chemotherapeutic agents [8]. DDP, as a broad spectrum antineoplastic agent in clinical practice, shows potent efficacies against a wide range of tumors because it can enhance the sensitivity of tumor cells to radiotherapy [9]; however, unfortunately, some patients who initially respond to DDP still develop drug resistance later [10, 11]. As well as other carcinomas, gene aberrations were believed to be the reason of the occurrence, progression, and treatment of NPC [12].

E2F transcription factors, which have been first identified as activators of the adenovirus E2 promoter, consist of E2F-1-8 [13]. E2F-1, the earliest discovered member of the E2F family cloned from Nalm6 and Akata cells, is important in regulating cell cycle distribution and proliferation [14]. To date, the role of E2F-1 in carcinogenesis is still controversial; E2F-1 can act as either an oncogene or tumor suppressor gene according to the published literature [15–17]. In NPC cancer tissues, E2F-1 was shown to be upregulated, which demonstrated a close correlation with the T stage of patients, and in vitro experiments also discovered much higher expression of E2F-1 in NPC cells than in normal nasopharyngeal epithelial cells (NP69) [18]. Exogenous expression of E2F-1 can further induce the expression of Stathmin1 (STMN1) in NPC-derived cells, whereas higher expression of STMN1 was reported to be associated with the poor prognosis of NPC patients [19]. Of note, the down-regulation of E2F-1 induced by resveratrol, the most well-known polyphenolic stilbenoid, can enhance the sensitivity of NPC cells to radiotherapy, suggesting that E2F-1 may act as an oncogene in NPC [20]. More importantly, E2F-1 was found to affect the sensitivity of tumor cells to DDP [21, 22].

In contrast, the upregulation of ataxia telangiectasia mutated (ATM), a protein belonging to the phosphatidylinositol 3-kinase (PI3K) family [23], and its overexpression were associated with worse overall survival of NPC [24]. ATM was also found to be relevant to the development of DDP resistance; in contrast, knockdown

of ATM can enhance the sensitivity of lung cancer cells and endometrial cancer cells to DDP [25, 26]. Moreover, ATM has been identified as a target for positive regulation by E2F-1 [27]. Therefore, we conducted in vitro and in vivo experiments to investigate whether E2F-1 plays a role in the development of DDP resistance in NPC via regulation of ATM.

## Materials and methods

### Cell culture

In this study, the DDP-resistant NPC cell line CNE2/DDP and its parental cell line CNE2 were provided by Shanghai Yiyan Biotechnology Co. Ltd. (China). In addition, HNE1/DDP and HNE1 cell lines were purchased from Beijing Beina Chuanglian Biotechnology Research Institute. CNE2 and HNE1 cells were maintained in RPMI-1640 medium supplemented with 10% fetal bovine serum (FBS) in 95% air and 5% CO<sub>2</sub> at 37°C. To maintain DDP resistance, CNE2/DDP and HNE1/DDP cells were cultured in RPMI 1640 medium containing 1% penicillin and streptomycin, 1 µg/mL DDP, 10% FBS at 37°C, and 5% CO<sub>2</sub> in a humidified incubator.

### Cell grouping and transfection

CNE2/DDP and HNE1/DDP cells were divided into the blank group (cells were not transfected), control shRNA group (cells were transfected with control short hairpin RNA plasmids, sc-108060, Santa Cruz Biotechnology, USA), E2F-1 shRNA#1 group (cells were transfected with E2F-1 shRNA plasmids, sc-44258, Santa Cruz Biotechnology, USA), E2F-1 shRNA#2 group (cells were transfected with E2F-1 shRNA plasmids, sc-29297, Santa Cruz Biotechnology, USA), ATM group (cells were transfected with ATM lentiviral activation particles, sc-400192-LAC, Santa Cruz Biotechnology, USA), E2F-1 shRNA#1 + ATM group (cells were cotransfected with E2F-1 shRNA plasmids and ATM lentiviral activation particles), and E2F-1 particles shRNA#2 + ATM group (cells were cotransfected with E2F-1 viral activation viral activation plasmids). Transfection procedures were performed using Lipofectamine<sup>TM</sup> 3000 Transfection Reagent (L3000015, Thermo Fisher, Shanghai, China).

### 3-(4,5-Dimethylthiazol-2-yl)-2,5-diphenyltetrazolium bromide (MTT) assay

Cells were harvested, centrifuged, digested, and diluted to  $2 \times 10^4$  cells/mL and then seeded evenly onto a 96-well plate. After confluence, cells in each well were treated with DDP at varying concentrations for 48 h, and the medium was discarded. In each well, 20 µL serum-free medium was added, followed by 4 h of incubation, and the supernatant was discarded. After incubation with slow shaking, crystals were

completely dissolved, and the optical density (OD) was determined at a wavelength of 490 nm. This experiment was repeated three times; the inhibition rate (%) =  $(1 - \text{OD value of treated group} / \text{OD value of the blank group}) \times 100\%$  [28]. The 50% inhibition concentration ( $IC_{50}$ ) and resistance index (RI) were calculated for the DDP-resistant NPC cell line, where  $RI = IC_{50}$  of the resistant line/ $IC_{50}$  of the parental cell line [29].

#### Cell cycle determined by flow cytometry

Cells were treated with 1 mg/mL RNase A at 37°C for 1 h followed by 5 mg/mL Proteinase K at 37°C for another 1 h. After washing with TE buffer, cells were resuspended in a SYBR Green I solution (Thermo Fisher Scientific, Waltham, MA, USA) at 4°C overnight. Flow cytometry (FACSCalibur; BD Biosciences, San Jose, CA, USA) and the IDEAS software version 6.2.187.0 (Merck KGaA, Darmstadt, Germany) were used to determine the phases of the cell cycle.

#### Cell proliferation assessed by Edu staining

An EdU incorporation assay was used to detect cell proliferation following the manufacturer's protocol (C103103, RiboBio, Guangzhou, China). Cells were stained with Apollo 567 to detect EdU (red) and 2-(4-amidinophenyl)-6-indolecarbamidine dihydrochloride (DAPI) (blue) to highlight nuclei, which were examined by fluorescence microscopy (Nikon Eclipse 80i; Nikon, Tokyo, Japan). The percentage of EdU<sup>+</sup> cells ( $\text{EdU}^+ / \text{DAPI}^+ \times 100$ ) was determined in 4 random fields per sample.

#### Quantitative real-time polymerase chain reaction (qRT-PCR)

According to the instructions of TRIzol Reagent (15596018; Thermo Fisher, China), total RNA was extracted from cells and subjected to cDNA synthesis using SuperScript IV Reverse Transcription (1809010; Thermo Fisher, China) with annealed RNA (50 μM random hexamer primers, 10 mM dNTP mix, 5 μg total RNA, DEPC-treated water) mixed with RT reaction mix (5 × SSIV Buffer, 100 mM DTT, RNaseOUT Recombinant RNase Inhibitor and SuperScript IV Reverse Transcriptase) at 50 °C for 10 min. cDNA was synthesized using total RNA. Expression of target genes was detected on an ABI7500 real-time fluorescent PCR apparatus with Power SYBR<sup>™</sup> Green PCR (4368706; Applied Biosystems, USA). The cycling conditions were an initial 10 min treatment at 95°C followed by 40 cycles of denaturation at 95°C for 15 s and annealing at 60°C for 1 min. Primer sequences are shown in Table 1, and the expression of target genes was calculated using the Formula  $2^{-\Delta\Delta C_t}$ .

#### Western blotting

Total proteins were extracted from cells using the TRIzol method (15596018, Invitrogen, USA), and following the determination of protein concentration and sodium dodecyl sulfate–polyacrylamide gel electrophoresis (SDS–PAGE, Thermo Scientific, Shanghai, China) for separation, proteins were transferred onto a polyvinylidene fluoride (PVDF, B1000B, Invitrogen, USA) membrane, on which the unoccupied sites were blocked in 5% nonfat milk. Proteins on the membrane were detected by incubation with E2F-1 antibody (ab137415, Abcam, USA) at a 1/500 dilution, ATM antibody (ab32420, Abcam, USA)

**Table 1** Primer sequences used in this study

Gene	GenBank Accession	Primer sequences (5'-3')
E2F-1	NM_005225	Forward Primer: ACGCTATGAGACCTCACTGAA Reverse Primer: TCCTGGGTCAACCCCTCAAG
ATM	NM_000051	Forward Primer: GGCTATTAGTGTGCGAGACA Reverse Primer: TGGCTCCTTTCGGATGATGGA
ABCA2	NM_001606	Forward Primer: GAGGAAGGCAACCTGTTTGAC Reverse Primer: GCAGCGACAAGTTTTCGT
ABCA5	NM_018672	Forward Primer: CTCTAAGCCGAGCACTTTGT Reverse Primer: ACAGCCAGCTCTTGAATCCAT
cyclin E1	NM_001238	Forward Primer: AAGGAGCGGGACACCATGA Reverse Primer: ACGGTCACGTTTGCTTCC
CDK2	NM_001798	Forward Primer: GTACCTCCCCTGGATGAAGAT Reverse Primer: CGAAATCCGCTTGTAGGGTC
GAPDH	NM_001256799	Forward Primer: CTGGGCTACACTGAGCACC Reverse Primer: AAGTGGTCGTTGAGGGCAATG

at a 1/3000 dilution, Ki67 antibody (ab92742, Abcam, USA) at a 1/5000 dilution, and  $\beta$ -actin antibody (ab8227, Abcam, USA) at 1  $\mu$ g/mL overnight at 4°C. The resulting immunoblots were incubated with secondary antibody at a 1/1000 dilution (Abcam, USA) for 1 h at room temperature. With  $\beta$ -actin as the loading control, the band intensity was analyzed using the ImageJ software (US National Institutes of Health, Bethesda, MD, USA). This experiment was repeated three times.

### Statistical analysis

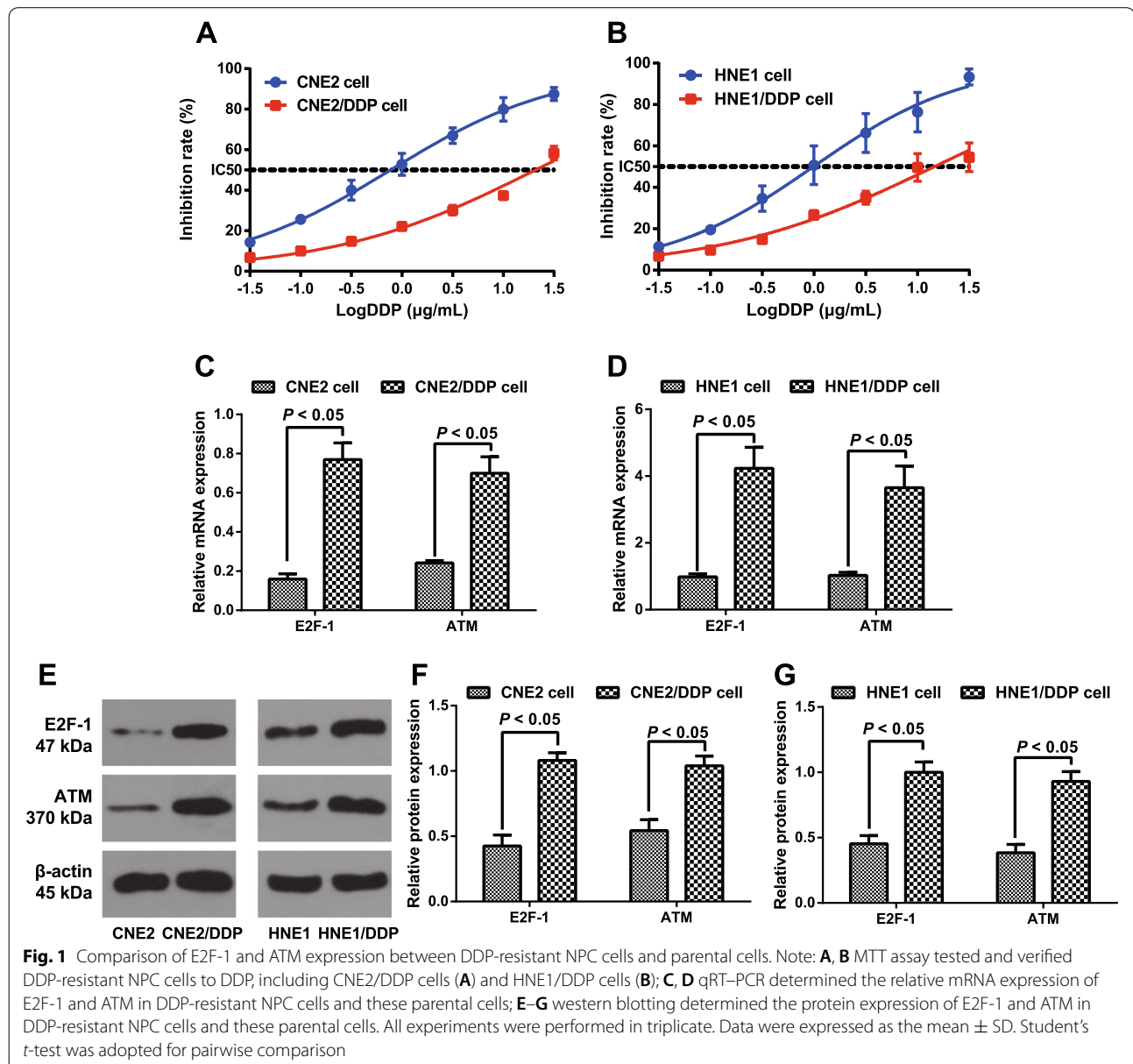
All data were subjected to statistical analysis in the Graph-Pad Software 6.0 (San Diego, CA, USA). Measurement

data are expressed as the mean  $\pm$  standard deviation (SD). A *t*-test was adopted for the comparison of measurement data, while analysis of variance was adopted for the comparison among several groups, followed by *Tukey's HSD* test for intragroup comparison.  $P < 0.05$  suggested that the difference was statistically significant.

## Results

### Comparison of E2F-1 and ATM expression

between DDP-resistant NPC cells and these parental cells First, DDP-resistant NPC cells (CNE2/DDP and HNE1/DDP) to DDP were tested and verified, and as a result analyzed by MTT assay (Fig. 1A, B); after treatment with



varying concentrations of DDP for 48 h, the  $IC_{50}$  values of CNE2 cells and CNE2/DDP cells were 0.77 and 20.81, respectively, with an RI of 27.03 for CNE2/DDP cells. Meanwhile, the  $IC_{50}$  values of HNE1 cells and HNE1/DDP cells were 0.99 and 14.56, respectively, with an RI of 14.71 for HNE1/DDP cells. In addition, qRT-PCR (Fig. 1C, D) and western blotting (Fig. 1E–G) demonstrated that the expression of E2F-1 and ATM in DDP-resistant NPC cells (CNE2/DDP and HNE1/DDP) was much higher than that in these parental cells (all  $P < 0.05$ ).

### Expression of E2F-1 and ATM in transfected DDP-resistant NPC cells

The expression of E2F-1 and ATM in CNE2/DDP and HNE1/DDP cells after transfection was detected via qRT-PCR (Fig. 2A) and western blotting (Fig. 2B, C) to further explore this relationship, and as a consequence, the transfection of E2F-1 shRNAs reduced the expression of E2F-1 and ATM in DDP-resistant NPC cells (all  $P < 0.05$ ). However, the transfection of ATM lentiviral activation particles significantly enhanced

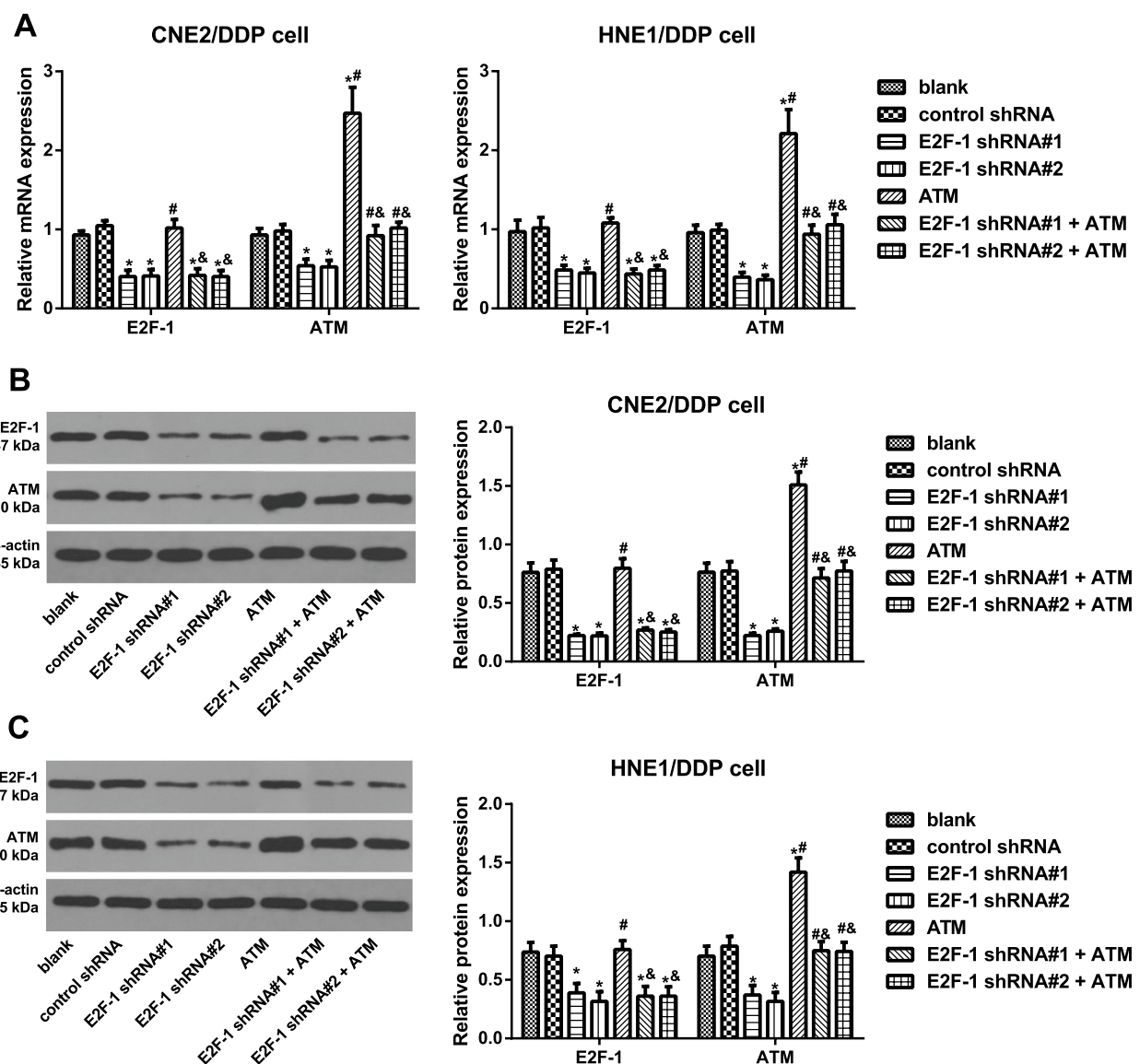


**Fig. 2** Expression of E2F-1 and ATM in transfected DDP-resistant NPC cells. Note: **A** qRT-PCR was used to determine the relative mRNA expression of E2F-1 and ATM in DDP-resistant NPC cells (CNE2/DDP and HNE1/DDP); **B**, **C** western blotting was used to determine the protein expression of E2F-1 and ATM in CNE2/DDP cells (**B**) and HNE1/DDP cells (**C**). The experiment was repeated independently three times. Comparisons among multiple groups were analyzed using one-way ANOVA, while intergroup differences were tested by Tukey's HSD test. \*,  $P < 0.05$  compared with the blank group and control shRNA group; #,  $P < 0.05$  compared with the E2F-1 shRNA#1 group and E2F-1 shRNA#2 group; &,  $P < 0.05$  compared with the ATM group



the expression of ATM without affecting E2F-1 expression, which was reversed by E2F-1 inhibition (all  $P < 0.05$ ).

#### E2F-1 downregulation increased the sensitivity of DDP-resistant NPC cells to DDP by regulating ATM

An MTT assay was employed to determine the  $IC_{50}$  values of CNE2/DDP and HNE1/DDP cells. As shown in Fig. 3A, B and Table 2, E2F-1 inhibition decreased the DDP resistance of DDP-resistant NPC cells, while ATM overexpression further enhanced DDP resistance. No significant difference was observed in the  $IC_{50}$  values and RI among the E2F-1 shRNA#1 + ATM group, E2F-1 shRNA#2 + ATM group, and control shRNA group. In addition, the expression of drug resistance-related genes,

including ATP binding cassette transporter-2 (ABCA2) and ABCA5, was also detected (Fig. 3C), and consequently, inhibition of E2F-1 reduced the expression of ABCA2 and ABCA5 in DDP-resistant NPC cells, while ATM overexpression showed the opposite changes, which could be further reversed by downregulation of E2F-1 (all  $P < 0.05$ ).

#### Effect of E2F-1 on the cycle distribution of DDP-resistant NPC cells via regulation of ATM

Through flow cytometry, E2F-1 downregulation was found to arrest the cycle of DDP-resistant NPC cells in the G1 phase, resulting in a decrease in cells in the S phase, while ATM overexpression induced elevations in the transition of the cells into the S phase. The effect of

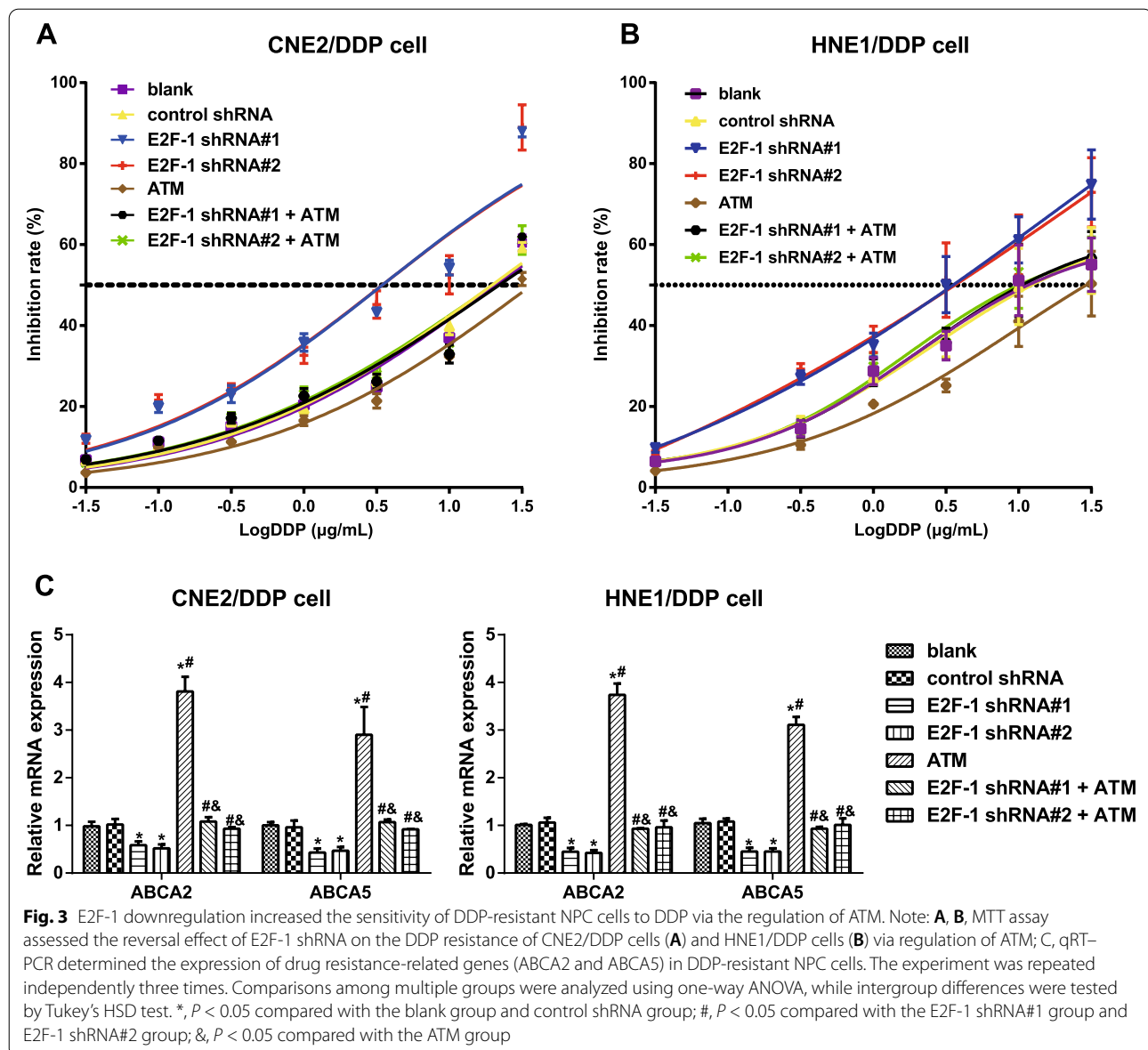


**Table 2** Reversal effect of E2F-1-downregulation on the DDP resistance of DDP-resistant NPC cells via regulation of ATM

	IC <sub>50</sub>	RI
CNE2 cell	0.77	
CNE2/DDP cell		
Blank	20.94	27.19
Control shRNA	19.67	25.55
E2F-1 shRNA#1	3.46	4.50
E2F-1 shRNA#2	3.46	4.49
ATM	36.90	47.92
E2F-1 shRNA#1 + ATM	22.07	28.66
E2F-1 shRNA#2 + ATM	20.07	26.06
HNE1 cell	0.99	-
HNE1/DDP cell		
Blank	13.25	13.38
Control shRNA	13.51	13.65
E2F-1 shRNA#1	3.34	3.37
E2F-1 shRNA#2	3.47	3.50
ATM	27.44	27.72
E2F-1 shRNA#1 + ATM	12.24	12.36
E2F-1 shRNA#2 + ATM	12.08	12.20

ATM lentiviral activation particles can be eliminated by the transfection of E2F-1 shRNA (Fig. 4A). The expression of the cycle-related genes cyclin E1 and cyclin-dependent kinase 2 (CDK2) in DDP-resistant NPC cells was further detected, and the results (Fig. 4B) showed that compared to the control shRNA group, the expression of cyclin E1 and CDK2 was downregulated after the inhibition of E2F-1 but upregulated after ATM overexpression (all  $P < 0.05$ ). In comparison with the ATM group, the expression of cyclin E1 and CDK2 was downregulated in the E2F-1 shRNA#1 + ATM group and E2F-1 shRNA#2 + ATM group (all  $P < 0.05$ ).

#### Effect of E2F-1 on the proliferation of DDP-resistant NPC cells via regulation of ATM

EdU staining was applied to measure the effect of E2F-1 on the proliferation of DDP-resistant NPC cells via regulation of ATM (Fig. 5A, B) and compared with the blank group; CNE2/DDP and HNE1/DDP cells decreased proliferation after transfection with E2F-1 shRNAs but increased proliferation with ATM lentiviral activation particles (both  $P < 0.05$ ), while those in the E2F-1 shRNA#1 + ATM group and E2F-1 shRNA#2 + ATM group showed no significant difference ( $P > 0.05$ ). In addition, the promoting effect of ATM overexpression on the expression of the proliferation marker Ki67 in DDP-resistant NPC cells was eliminated by downregulation of E2F-1 ( $P < 0.05$ ), as determined by western blotting (Fig. 5C, D).

#### Discussion

In our study, we first found that the mRNA and protein expression of E2F-1 in DDP-resistant NPC cells was much higher than that in these parental cells. In agreement with our findings, Zheng, H et al. also observed the upregulation of E2F-1 in gastric cancer cells after treatment with paclitaxel and DDP [22]. The results presented here showed a correlation of E2F-1 with the resistance of tumor cells to DDP; thus, we speculated that E2F-1 inhibition may be a potential target to reverse the DDP resistance of NPC cells. As reported, the Tip60/E2F-1 complex stabilizing E2F-1 by acetylation at lysine residues 120 and 125 controlled the accumulation of enzyme excision repair cross-complementing Group 1 (ERCC1), which is known to play a rate-limiting role in the repair of platinum (e.g., DDP)-DNA adducts [30]. D-Arg PEP, as an inhibitor of E2F transcription, in combination with DDP enhances DNA damage, demonstrating synergistic inhibition of androgen-sensitive and castration-resistant prostate cells, breast cancer cells, and lymphoma cells [21]. In addition, E2F-1 could induce drug resistance by targeting ABCA2 and ABCA5 in the study of Vijay Alla et al. [31]. However, the decline in the transcriptional activity of E2F-1 contributed to reversing multidrug resistance [32]. Thus, the DDP-resistant NPC cells in the following experiments were transfected with E2F-1 shRNAs to inhibit the expression of E2F-1, and such transfection could reduce the IC<sub>50</sub> value of cells to DDP, with a decreased RI and downregulation of drug resistance-related genes (ABCA2 and ABCA5), which verified our assumption, and similar results were reported in previous studies.

Here, DDP-resistant NPC cells transfected with E2F-1 shRNAs were also found to be able to arrest cells in the G1 phase of the cell cycle. The possible mechanism was that E2F-1 was credited as a master regulator of restriction (R) point and S phase transit, and its activity was released in the late G1 phase, triggered by dissociation from retinoblastoma protein (pRb) [33, 34]. Additionally, the microinjection of E2F-1 cDNA, as reported, could induce quiescent cells into the S phase [35]. Similarly, silencing E2F-1 could, directly or indirectly, downregulate the expression of drug resistance-related genes to prevent cells from entering the S phase, finally reversing the multidrug resistance of gastric cancer cells [36, 37]. In addition, S Inoshita et al. found that E2F-1 was essential in the G1/S transition, which could advance the cell cycle by inducing the expression of cyclin D1 and cyclin E [38]. In addition, Huang Y et al. also suggested that palbociclib could enhance the antitumor effect of DDP by regulating the cyclin D1/RB/E2F-1 axis [39]. Therefore, we detected the expression of downstream targets of E2F-1, including cyclin E1 and CDK2 [40–43], and consequently, E2F-1

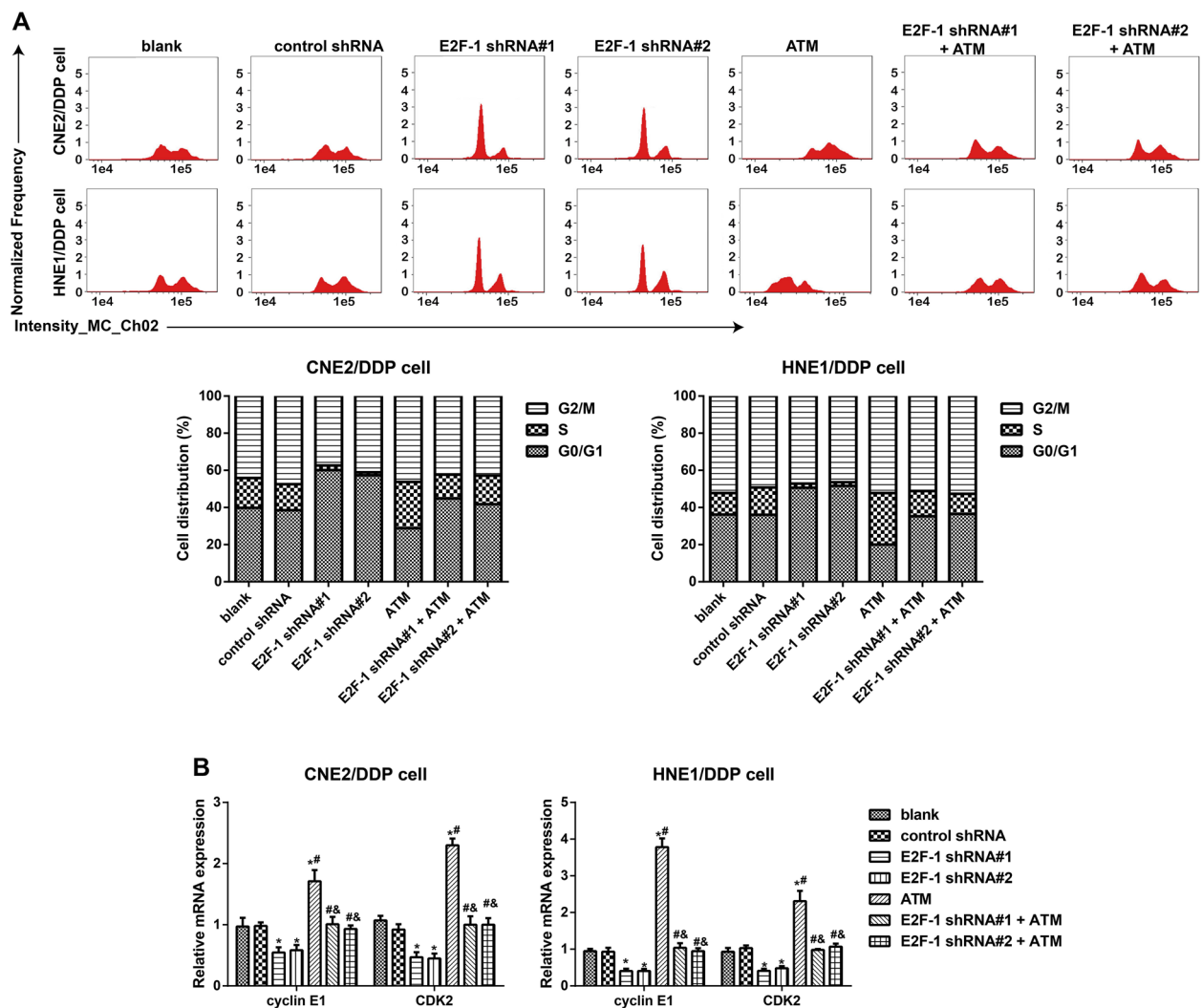


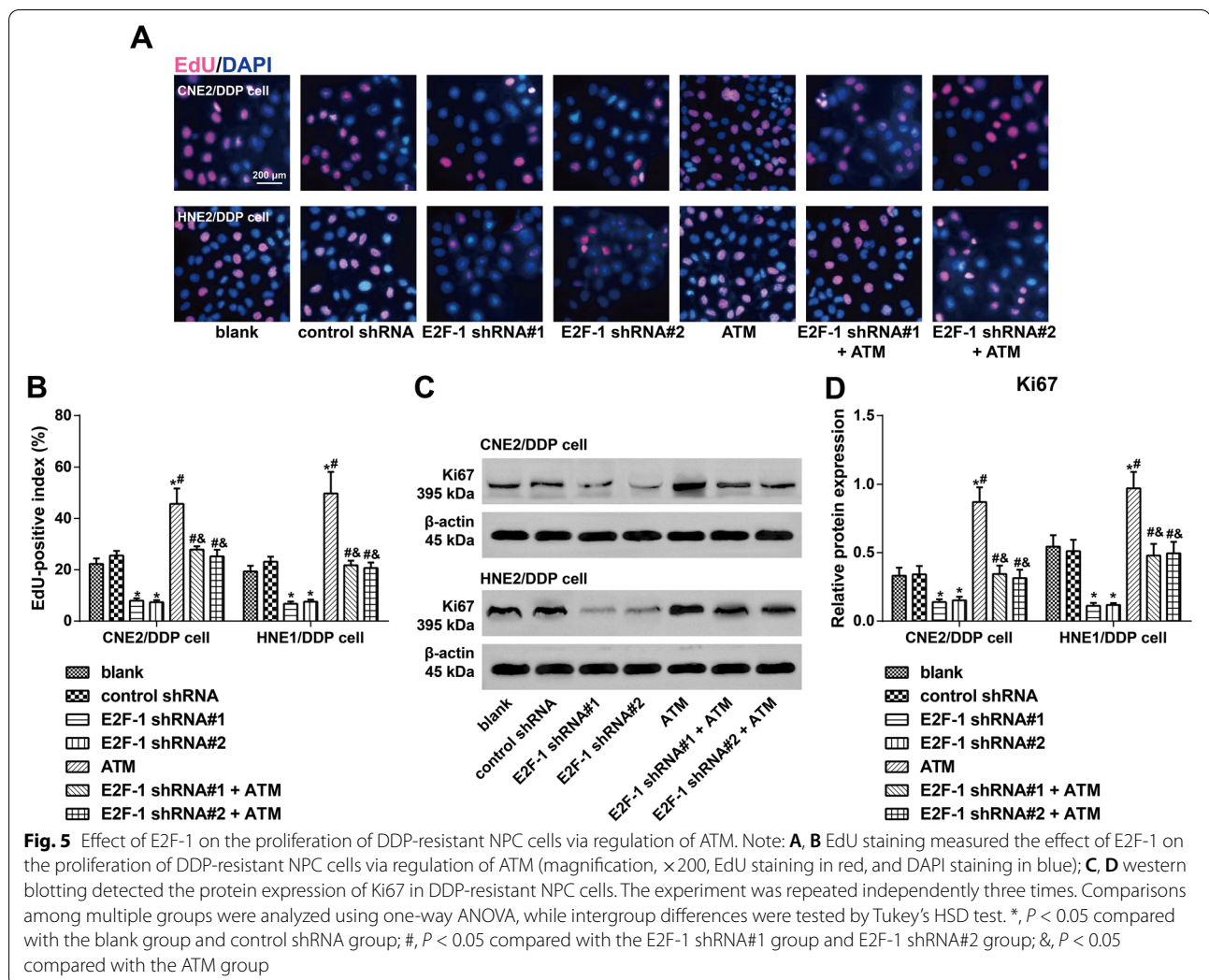
**Fig. 4** Effect of E2F-1 on the cycle distribution of DDP-resistant NPC cells via regulation of ATM. Note: **A** Flow cytometry evaluated the effect of E2F-1 on the cycle distribution of DDP-resistant NPC cells via regulation of ATM; **B** qRT-PCR determined the expression of cycle-related genes (cyclin E1 and CDK2) in DDP-resistant NPC cells; the experiment was repeated independently three times. Comparisons among multiple groups were analyzed using one-way ANOVA, while intergroup differences were tested by Tukey's HSD test. \*,  $P < 0.05$  compared with the blank group and control shRNA group; #,  $P < 0.05$  compared with the E2F-1 shRNA#1 group and E2F-1 shRNA#2 group; &,  $P < 0.05$  compared with the ATM group

downregulation further reduced the expression of cyclin E1 and CDK2 in DDP-resistant NPC cells.

From this study, we found that inhibition of E2F-1 could also obviously reduce the proliferation of DDP-resistant NPC cells, with the significant down-regulation of Ki67. Previous study demonstrated that E2F-1 overexpression in lung tumors and nonfamilial retinoblastoma were significantly associated with a high Ki67 index [44, 45], a well-known proliferation marker for the evaluation of cell proliferation [46], suggesting that E2F-1 may block the DDP-resistant NPC cell cycle in G1 phase to reduce the proliferation of cells and enhance the sensitivity to DDP.

ATM, closely related to cell cycle checkpoint control [47], was also increased in DDP-resistant NPC cells compared with the parental cells, which was similar to previous studies, and inhibition of ATM could enhance the sensitivity of DDP-resistant cells to DDP [25, 48, 49]. The use of KU-60019, an inhibitor of ATM, could increase the sensitivity of PTEN-deficient breast cancer cells to DDP [50]. Additionally, the transcription factor forkhead box M1 (FoxM1) could increase the sensitivity of NPC cells to DDP by inhibiting the Mre11-Rad50-Nbs1 (MRN)-ATM axis [51]. ATM dysfunction results in abnormal checkpoint responses in multiple phases of the cell cycle, including G1, S, and G2 [47]. For example, inhibiting the





activation of pathways between ATM and ATR could enhance the sensitivity of cancer cells to chemotherapeutics [52]. In our work, ATM overexpression promoted the transition of DDP-resistant NPC cells into S phase, with a significant increase in proliferation, and as a result, the  $IC_{50}$  to DDP was also increased, suggesting more severe resistance to drugs, which was also verified by the upregulation of ABCA2 and ABCA5.

Finally, the transfection of ATM lentiviral activation particles could significantly enhance the expression of ATM without any significant effects on the expression of E2F-1; however, the effect of ATM overexpression on DDP-resistant NPC cells was reversed by E2F-1 shRNA, indicating that E2F-1 may modulate the sensitivity of DDP-resistant NPC cells by regulating ATM. ATM, which plays an essential role in DSB repair, can be a potential target of cancer chemotherapy, including DDP [53]. The nt sequence of the human *ATM* promoter contains several E2F consensus sites and can be

directly transactivated by E2F-1 [27]. Tumor suppressor bridging integrator 1 (BIN1)-dependent E2F-1 repression may be a mechanism by which BIN1 reduces ATM levels, and the increased DDP resistance induced by BIN1 deficiency was conversely eliminated by ATM inactivation or E2F-1 reduction [54]. Previous studies have also uncovered that E2F-1 transcriptionally activates ATM, which is the main cellular sensor of DNA damage, representing a potential therapeutic tool for DDP resistance [55], indicating that E2F-1 may affect the sensitivity of DDP-resistant NPC cells to DDP via positive regulation of ATM.

However, there were some limitations in the current study. First, animal or tissue verification experiments were not performed, resulting in the difficulty of making a solid conclusion. Second, additional pathway analysis and additional data with other platinum should be further explored. The main strength of this study was that we uncovered a potentially novel mechanism by which

E2F-1 regulated ATM and mediated DDP resistance in NPC. In addition, we used multiple cell lines and shRNAs to confirm our results.

In conclusion, E2F-1 and ATM expression in DDP-resistant NPC cells was much higher than that in these parental cells. Inhibition of E2F-1, possibly through suppression of ATM, blocked DDP-resistant NPC cells at the G1 phase with reduced cell proliferation, thereby reversing the resistance of human NPC cells to DDP.

#### Acknowledgements

The authors appreciate the reviewers for their useful comments in this paper.

#### Authors' contributions

Zun-Yan Zhou designed the study; Ji-Yuan Yang carried out experiments; Cheng-Ze Shao analyzed the data; Fei Luo made the figures; Wei Du drafted and revised the paper; the authors read and approved the final version of the manuscript.

#### Funding

There was no funding in this study.

#### Availability of data and materials

The data that support the findings of this study are available on request form the corresponding author. The data are not publicly available due to privacy.

#### Declarations

##### Ethics approval and consent to participate

Ethical approval was not required for this study in accordance with local/national guidelines.

##### Consent for publication

Written informed consent from participants was not required in accordance with local/national guidelines.

##### Competing interests

The authors declare that they have no competing interests.

Received: 5 December 2021 Accepted: 28 February 2022

Published online: 18 March 2022

#### References

- Hao W, Wu L, Cao L, Yu J, Ning L, Wang J, et al. Radioresistant nasopharyngeal carcinoma cells exhibited decreased cisplatin sensitivity by inducing SLC1A6 expression. *Front Pharmacol*. 2021;12:629264.
- Yan Z, Lijuan Y, Yinhang W, Yin J, Jiamin X, Wei W, et al. Screening and analysis of RNAs associated with activated memory CD4 and CD8 T cells in liver cancer. *World J Surg Oncol*. 2022;20:2.
- Kang Y, He W, Ren C, Qiao J, Guo Q, Hu J, et al. Advances in targeted therapy mainly based on signal pathways for nasopharyngeal carcinoma. *Signal Transduct Target Ther*. 2020;5:245.
- Zheng M, Liu J, Meng C, Tang K, Liao J. Prognostic and clinicopathological importance of microRNA-140 expression in cancer patients: a meta-analysis. *World J Surg Oncol*. 2021;19:266.
- Cai J, Zhou M, Xu J. N6-methyladenosine (m6A) RNA methylation regulator SNRPC is a prognostic biomarker and is correlated with immunotherapy in hepatocellular carcinoma. *World J Surg Oncol*. 2021;19:241.
- Mu W, Xie Y, Li J, Yan R, Zhang J, Liu Y, et al. High expression of PDZ-binding kinase is correlated with poor prognosis and immune infiltrates in hepatocellular carcinoma. *World J Surg Oncol*. 2022;20:22.
- Pfister DG, Spencer S, Adelstein D, Adkins D, Anzai Y, Brizel DM, et al. Head and Neck Cancers, Version 2.2020, NCCN Clinical Practice Guidelines in Oncology. *J Natl Compr Canc Netw*. 2020;18:873–98.
- Lee AW, Lin JC, Ng WT. Current management of nasopharyngeal cancer. *Semin Radiat Oncol*. 2012;22:233–44.
- Brown A, Kumar S, Tchounwou PB. Cisplatin-based chemotherapy of human cancers. *J Cancer Sci Ther*. 2019;11(4):97.
- Wang K, Chen Z, Long L, Tao Y, Wu Q, Xiang M, et al. iTRAQ-based quantitative proteomic analysis of differentially expressed proteins in chemoresistant nasopharyngeal carcinoma. *Cancer Biol Ther*. 2018;19:809–24.
- Kuang CM, Fu X, Hua YJ, Shuai WD, Ye ZH, Li Y, et al. BST2 confers cisplatin resistance via NF-kappaB signaling in nasopharyngeal cancer. *Cell Death Dis*. 2017;8:e2874.
- Mou T, Zhu D, Wei X, Li T, Zheng D, Pu J, et al. Identification and interaction analysis of key genes and microRNAs in hepatocellular carcinoma by bioinformatics analysis. *World J Surg Oncol*. 2017;15:63.
- Liao P, Han S, Qu H. Expression, prognosis, and immune infiltrates analyses of E2Fs in human brain and CNS cancer. *Biomed Res Int*. 2020;2020:6281635.
- Wu ZH, Yun T, Cheng Q. Data mining identifies six proteins that can act as prognostic markers for head and neck squamous cell carcinoma. *Cell Transplant*. 2020;29:963689720929308.
- Fouad S, Hauton D, D'Angiolella V. E2F1: cause and consequence of DNA replication stress. *Front Mol Biosci*. 2020;7:599332.
- El Dika M. Redirecting E2F1 to TA-p73 improves cancer therapy through apoptotic induction. *DNA Repair (Amst)*. 2020;90:102858.
- Chun JN, Cho M, Park S, So I, Jeon JH. The conflicting role of E2F1 in prostate cancer: a matter of cell context or interpretational flexibility? *Biochim Biophys Acta Rev Cancer*. 2020;1873:188336.
- Liu P, Zhang X, Li Z, Wei L, Peng Q, Liu C, et al. A significant role of transcription factors E2F in inflammation and tumorigenesis of nasopharyngeal carcinoma. *Biochem Biophys Res Commun*. 2020;524:816–24.
- Hsu HP, Li CF, Lee SW, Wu WR, Chen TJ, Chang KY, et al. Overexpression of stathmin 1 confers an independent prognostic indicator in nasopharyngeal carcinoma. *Tumour Biol*. 2014;35:2619–29.
- Tan Y, Wei X, Zhang W, Wang X, Wang K, Du B, et al. Resveratrol enhances the radiosensitivity of nasopharyngeal carcinoma cells by downregulating E2F1. *Oncol Rep*. 2017;37:1833–41.
- Rather GM, Anyanwu M, Minko T, Garbuzenko O, Szekely Z, Bertino JR. Anti-tumor effects of a penetratin peptide targeting transcription of E2F-1, 2 and 3a is enhanced when used in combination with pemetrexed or cisplatin. *Cancers (Basel)*. 2021;13(5):972.
- Zheng H, Wang JJ, Yang XR, Yu YL. Upregulation of miR-34c after silencing E2F transcription factor 1 inhibits paclitaxel combined with cisplatin resistance in gastric cancer cells. *World J Gastroenterol*. 2020;26:499–513.
- Yan M, Tang C, Ma Z, Huang S, Dong Z. DNA damage response in nephrotoxic and ischemic kidney injury. *Toxicol Appl Pharmacol*. 2016;313:104–8.
- Ko JJ, Klimowicz AC, Jagdis A, Phan T, Laskin J, Lau HY, et al. ATM, THMS, and RRM1 protein expression in nasopharyngeal carcinomas treated with curative intent. *Head Neck*. 2016;38(Suppl 1):E384–91.
- Shen M, Xu Z, Xu W, Jiang K, Zhang F, Ding Q, et al. Inhibition of ATM reverses EMT and decreases metastatic potential of cisplatin-resistant lung cancer cells through JAK/STAT3/PD-L1 pathway. *J Exp Clin Cancer Res*. 2019;38:149.
- Takeuchi M, Tanikawa M, Nagasaka K, Oda K, Kawata Y, Oki S, et al. Anti-tumor effect of inhibition of DNA damage response proteins, ATM and ATR, in endometrial cancer cells. *Cancers (Basel)*. 2019;11(12):1913.
- Berkovich E, Ginsberg D. ATM is a target for positive regulation by E2F-1. *Oncogene*. 2003;22:161–7.
- Chang ZW, Jia YX, Zhang WJ, Song LJ, Gao M, Li MJ, et al. LncRNA-TUSC7/miR-224 affected chemotherapy resistance of esophageal squamous cell carcinoma by competitively regulating DESC1. *J Exp Clin Cancer Res*. 2018;37:56.
- Gaspar N, Sharp SY, Pacey S, Jones C, Walton M, Vassal G, et al. Acquired resistance to 17-allylamino-17-demethoxygeldanamycin (17-AAG, tane-spimycin) in glioblastoma cells. *Cancer Res*. 2009;69:1966–75.
- Putzer BM, Engelmann D. E2F1 apoptosis counterattacked: evil strikes back. *Trends Mol Med*. 2013;19:89–98.
- Alla V, Kowtharapu BS, Engelmann D, Emmrich S, Schmitz U, Steder M, et al. E2F1 confers anticancer drug resistance by targeting ABC transporter family members and Bcl-2 via the p73/DNp73-miR-205 circuitry. *Cell Cycle*. 2012;11:3067–78.

32. Dong Z, Ren L, Lin L, Li J, Huang Y, Li J. Effect of microRNA-21 on multidrug resistance reversal in A549/DDP human lung cancer cells. *Mol Med Rep.* 2015;11:682–90.
33. Stevens C, La Thangue NB. E2F and cell cycle control: a double-edged sword. *Arch Biochem Biophys.* 2003;412:157–69.
34. Wang A, Li CJ, Reddy PV, Pardee AB. Cancer chemotherapy by deoxynucleotide depletion and E2F-1 elevation. *Cancer Res.* 2005;65:7809–14.
35. Johnson DG, Schwarz JK, Cress WD, Nevins JR. Expression of transcription factor E2F1 induces quiescent cells to enter S phase. *Nature.* 1993;365:349–52.
36. Lian C, Yang J, Wang X, Xie Y, Xiao Q. Reversion of multidrug resistance of human gastric cancer SGC7901/DDP cells by E2F-1 gene silencing. *Zhonghua Zhong Liu Za Zhi.* 2014;36:171–6.
37. Yan LH, Wang XT, Yang J, Kong FB, Lian C, Wei WY, et al. Reversal of multidrug resistance in gastric cancer cells by E2F-1 downregulation in vitro and in vivo. *J Cell Biochem.* 2014;115:34–41.
38. Inoshita S, Terada Y, Nakashima O, Kuwahara M, Sasaki S, Marumo F. Regulation of the G1/S transition phase in mesangial cells by E2F1. *Kidney Int.* 1999;56:1238–41.
39. Huang Y, Wu H, Li X. Novel sequential treatment with palbociclib enhances the effect of cisplatin in RB-proficient triple-negative breast cancer. *Cancer Cell Int.* 2020;20:501.
40. Gu Y, Wang X, Liu H, Li G, Yu W, Ma Q. SET7/9 promotes hepatocellular carcinoma progression through regulation of E2F1. *Oncol Rep.* 2018;40:1863–74.
41. Chang MM, Lai MS, Hong SY, Pan BS, Huang H, Yang SH, et al. FGF9/FGFR2 increase cell proliferation by activating ERK1/2, Rb/E2F1, and cell cycle pathways in mouse Leydig tumor cells. *Cancer Sci.* 2018;109:3503–18.
42. Xu G, Meng Y, Wang L, Dong B, Peng F, Liu S, et al. miRNA-214-5p inhibits prostate cancer cell proliferation by targeting SOX4. *World J Surg Oncol.* 2021;19:338.
43. Yang H, Huo J, Li X. Identification and validation of a five-gene prognostic signature for hepatocellular carcinoma. *World J Surg Oncol.* 2021;19:90.
44. Eymen B, Gazzeri S, Brambilla C, Brambilla E. Distinct pattern of E2F1 expression in human lung tumours: E2F1 is upregulated in small cell lung carcinoma. *Oncogene.* 2001;20:1678–87.
45. Orjuela M, Orlow I, Dudas M, Ponce-Castaneda MV, Ridaura C, Leal C, et al. Alterations of cell cycle regulators affecting the RB pathway in nonfamilial retinoblastoma. *Hum Pathol.* 2001;32:537–44.
46. Yang C, Zhang J, Ding M, Xu K, Li L, Mao L, et al. Ki67 targeted strategies for cancer therapy. *Clin Transl Oncol.* 2018;20:570–5.
47. Pandita TK, Lieberman HB, Lim DS, Dhar S, Zheng W, Taya Y, et al. Ionizing radiation activates the ATM kinase throughout the cell cycle. *Oncogene.* 2000;19:1386–91.
48. Yan W, Yang Y, Yang W. Inhibition of SKP2 activity impaired ATM-mediated DNA repair and enhanced sensitivity of cisplatin-resistant mantle cell lymphoma cells. *Cancer Biother Radiopharm.* 2019;34:451–8.
49. Zhang F, Shen M, Yang L, Yang X, Tsai Y, Keng PC, et al. Simultaneous targeting of ATM and Mcl-1 increases cisplatin sensitivity of cisplatin-resistant non-small cell lung cancer. *Cancer Biol Ther.* 2017;18:606–15.
50. Li K, Yan H, Guo W, Tang M, Zhao X, Tong A, et al. ATM inhibition induces synthetic lethality and enhances sensitivity of PTEN-deficient breast cancer cells to cisplatin. *Exp Cell Res.* 2018;366:24–33.
51. Li D, Ye L, Lei Y, Wan J, Chen H. Downregulation of FoxM1 sensitizes nasopharyngeal carcinoma cells to cisplatin via inhibition of MRN-ATM-mediated DNA repair. *BMB Rep.* 2019;52:208–13.
52. Iwata T, Uchino T, Koyama A, Johmura Y, Koyama K, Saito T, et al. The G2 checkpoint inhibitor CBP-93872 increases the sensitivity of colorectal and pancreatic cancer cells to chemotherapy. *PLoS One.* 2017;12:e0178221.
53. Weber AM, Ryan AJ. ATM and ATR as therapeutic targets in cancer. *Pharmacol Ther.* 2015;149:124–38.
54. Folk WP, Kumari A, Iwasaki T, Pyndiah S, Johnson JC, Cassimere EK, et al. Loss of the tumor suppressor BIN1 enables ATM Ser/Thr kinase activation by the nuclear protein E2F1 and renders cancer cells resistant to cisplatin. *J Biol Chem.* 2019;294:5700–19.
55. Cataldo A, Cheung DG, Balsari A, Tagliabue E, Coppola V, Iorio MV, et al. miR-302b enhances breast cancer cell sensitivity to cisplatin by regulating E2F1 and the cellular DNA damage response. *Oncotarget.* 2016;7:786–97.

## Publisher's Note

Springer Nature remains neutral with regard to jurisdictional claims in published maps and institutional affiliations.

**Ready to submit your research? Choose BMC and benefit from:**

- fast, convenient online submission
- thorough peer review by experienced researchers in your field
- rapid publication on acceptance
- support for research data, including large and complex data types
- gold Open Access which fosters wider collaboration and increased citations
- maximum visibility for your research: over 100M website views per year

**At BMC, research is always in progress.**

Learn more [biomedcentral.com/submissions](https://biomedcentral.com/submissions)

